

Long Range Order in Two Dimensional Fractal Aggregation

D. J. Robinson and J. C. Earnshaw

The Department of Pure and Applied Physics, The Queen's University of Belfast, Belfast BT7 1NN, Northern Ireland

(Received 15 March 1993)

Long range intercluster structural order has been observed in the late, diffusion-limited stages of cluster-cluster aggregation of colloidal monolayers at liquid surfaces. The structure factor $S(q, t)$ scales as $q_m^{-d_f}(t)F(q/q_m)$, the exponent being the fractal dimension of two dimensional diffusion-limited cluster aggregation. Such scaling is not observed when the aggregation is reaction limited.

PACS numbers: 64.75.+g, 05.40.+j, 64.60.Ht, 82.70.Dd

Nonequilibrium processes in colloidal systems have excited much recent interest, particularly concerning the structural and kinetic aspects of aggregation. The fractal nature of structures formed in cluster-cluster aggregation has been demonstrated, the extremes of diffusion (DLCA) and reaction limited (RLCA) aggregation having both been observed, and the critical scaling predicted for the aggregation kinetics has been confirmed [1]. However, the recent report that aggregation in three dimensional colloidal suspensions of rather high volume fractions exhibits features similar to systems undergoing spinodal decomposition [2] was completely unexpected, suggesting the need for some reassessment of our understanding of the fundamental processes involved. This Letter presents the first measurements of such dynamics in the aggregation of two dimensional colloidal monolayers.

While spinodal decomposition (SD) may not be strictly relevant to these colloidal processes, a brief summary of the main features of this process is useful. Conventionally, spinodal decomposition is the mechanism by which phase separation occurs in a mixture that is quenched into a thermodynamically unstable state. The characteristic range of unstable concentration fluctuations and the formally negative diffusion coefficient lead to a fastest growing fluctuation at finite wave number, producing a ring in the pattern of scattered radiation, the radius of which changes with time. Despite the diversity of the physical systems in which SD has been observed [3], universal features are found in the kinetics. Furukawa [4] has shown that in the later, nonlinear stages the structure factor $S(q, t)$ scales according to a universal law,

$$S(q/q_m, t) = q_m^{-d}(t)F(q/q_m), \quad (1)$$

where q_m is the position of the structure factor peak and $S(q/q_m, t)$ is the structure factor. $F(q/q_m)$ is a time independent scaling function. Normally the exponent in this relation is just d , the dimension of the space in which the system is embedded. Such scaling of $S(q, t)$ has been observed in a variety of systems in which SD plays no part (e.g., breath figures [5]), suggesting it may be a more general feature of the coarsening process.

A colloidal system may be "quenched" into a region

of instability by the addition of an electrolyte which effectively screens the electrostatic repulsion between the colloidal particles. The ensuing aggregation apparently exhibits scaling features similar to those proposed by Furukawa [2], despite the lack of anomalous diffusion of monomers and clusters in the unstable region. In dense suspensions exhibiting DLCA the structure factor $S(q)$ scales as in Eq. (1), but with an exponent equal to d_f , the fractal dimension of the colloidal clusters, rather than d .

The surprising similarities between these observations and certain aspects of SD in conventional systems appear to suggest some underlying common mechanism in the dynamics of these irreversible processes. Quantitative studies are needed to study the dependence of the coarsening process on the aggregation kinetics to further test these ideas. For example, there is a need to investigate this effect in embedding spaces of different dimensionality. For two dimensional (2D) colloidal monolayers trapped at a liquid surface [6] the structure can be directly visualized by optical microscopy; the correlations between the clusters can easily be seen. Further, the high density limit of cluster-cluster aggregation can also be realized and studied more easily than in 3D, phase separation under the action of gravity is precluded, and the aggregates are less liable to mechanical instability induced by bending or hydrodynamic stress.

Our experimental methods have been described in full elsewhere [6(a)]. In brief, polystyrene latex spheres of $\sim 1 \mu\text{m}$ diameter (Seragen Diagnostics Ltd.) were spread on the surface of an aqueous subphase. Monolayer area fractions (ϕ) were rather high, typically $\approx 10\%$. The particles are highly charged and interact via long range dipole-dipole electrostatic forces [7]. Adding salt (CaCl_2) to the subphase induced irreversible aggregation, which proceeded to gelation over times of the order of several hours. Images were grabbed at various stages throughout aggregation for subsequent analysis.

Figure 1 shows a sequence of images taken as a colloidal monolayer aggregated on a $0.73M$ subphase. Such a sequence represents quasirandomly selected samples, due to some mobility of the colloidal monolayers [6(a)]. The images typically contain some 19 000 clusters at early times, falling to about 250 just prior to gelation. Clearly,

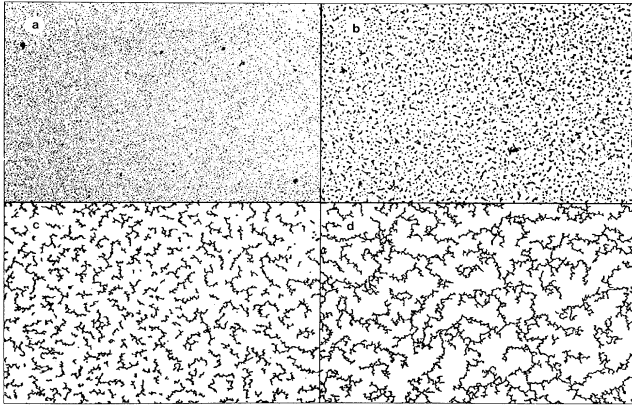


FIG. 1. Four digitized pictures ($730 \times 486 \mu\text{m}$) of a colloidal monolayer on a $0.73M$ CaCl_2 substrate at different times after initiation of aggregation: (a) 15, (b) 75, (c) 105, and (d) 135 min.

over length scales of the order of the cluster sizes the aggregates are fractal (Fig. 1). The fractal dimension found by the sandbox method [6(a)], $d_f = 1.43 \pm 0.04$, corresponded to values found in simulations of DLCA in 2D. At larger length scales the clusters appear roughly equally spaced, their separations increasing with time (Fig. 1).

More quantitative analysis supports this latter point. The separations of nearest neighbor clusters in such images were determined from the Delaunay triangulation [8] of the centers of gravity of all clusters not intersecting the image boundary. Probability distributions of these separations [$P(x)$] are shown in Fig. 2. During aggregation the distribution moves bodily to larger x , widening somewhat as it does so, in qualitative accord with expectation for Eq. (1). Error bars are small enough that the distributions are distinct, but are omitted from Fig. 2 for clarity. They may be estimated from the numbers of clusters on which each image is based (see caption).

Equation (1) applies in Fourier transform (FT) space, so the power spectra of the binary experimental micrographs were computed (as the square modulus of their 2D FT), and the structure factors $S(q, t)$ obtained by angular averaging. Figure 3 shows a series of $S(q, t)$; as aggregation proceeds and clusters begin to form the structure factor develops a peak at finite q . As cluster growth continues, the peak shifts to smaller q and its width decreases. At gelation the maximum in $S(q, t)$ merged with the $q = 0$ peak to assume a monotonic decay, reflecting the fractal nature of the gelling structure. The results presented here relate to earlier times. At large q , $S(q, t)$ tends to a single asymptotic curve (inset of Fig. 3) decaying as a power law in q , consistent with the fractal dimension given above. The position of the peak (q_m) in $S(q, t)$ correlates well with the maximum (x_m) of $P(x)$: $q_m \approx 2\pi/x_m$. We do not pursue this in detail as there is no direct one-to-one relation between

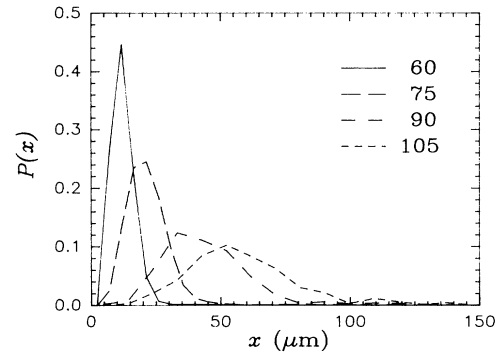


FIG. 2. Probability distributions of the separations of nearest neighbors in the colloidal monolayer of Fig. 1. The legend indicates times (in minutes) after initiation of aggregation. The distributions derive from 2907, 948, 214, and 170 clusters (in order of increasing time).

$P(x)$ and $S(q, t)$. The ability to simultaneously study structure in both real and Fourier space is, however, a major advantage of 2D colloidal systems.

Equation (1), embodying the scaling formalism of Furukawa, shows that the structure function $S(q, t)$ scales with a single length parameter. Figure 4 shows that rescaling by q_m does indeed lead to the collapse of the later $S(q/q_m, t)$ of Fig. 3 onto a scaling form $F(q/q_m)$. The scaling exponent was found to be the fractal dimension of the system ($d_f = 1.43$); a variation of more than $\approx 7\%$ from this value leads to a noticeable degradation of the reduction to a single curve. It would appear that the scaling exponent for coarsening in 2D colloidal aggregation is the fractal dimension of the system. While the large q dependence of $S(q, t)$ upon d_f is established, the influence of d_f upon the intercluster separation, reflected in q_m , is less obvious. The scaling of $S(q, t)$ as in Eq. (1), with d_f in place of d , suggests that in some sense such

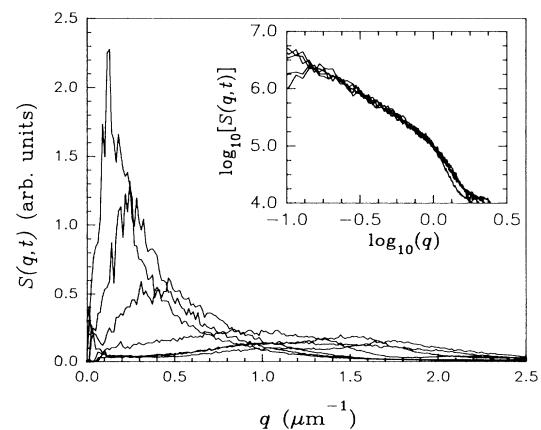


FIG. 3. Plots of the structure factor at times from 15 to 105 min after initiation of aggregation for the system of Fig. 1. Inset: a log-log plot of the high q data, demonstrating the fractal scaling at short length scales.

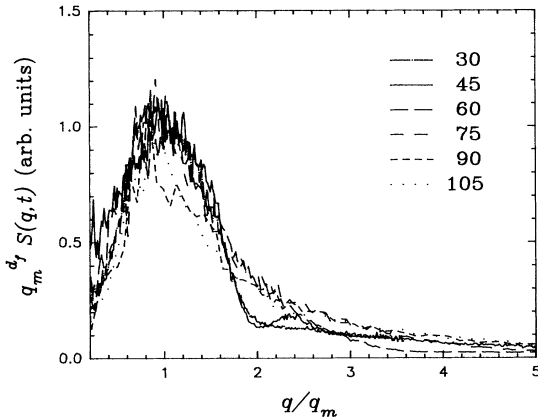


FIG. 4. The structure factors of Fig. 3 rescaled as $q_m^{d_f}(t)S(q/q_m, t)$. The data are for the later stages of aggregation only (times as legend).

systems exist in a space of dimensionality d_f , so that the fractal concept provides a way of interpolating between Euclidean spaces of different dimensionality.

The $S(q, t)$ characterizing the early stages of aggregation do not scale spinodally; in particular they do not grow exponentially at fixed q_m as expected from the linear Cahn-Hilliard theory [9]. This is also observed in bulk colloidal suspensions [2]. This likely arises from the inapplicability of this theory to these systems. However, it may also be, at least in part, because scaling in colloidal aggregation is specific to the diffusion-limited case [10]. In the earlier stages of aggregation the structure and kinetics resemble those for RLCA [6(b)] (as in 3D [11]). The kinetics can be typified by the average cluster size $s(t)$: Initially $s(t)$ grows slowly, being reaction limited, but at large times it increases faster, asymptotically as $s(t) \propto t^z$, where the scaling exponent z increases monotonically with subphase molarity [6(b)]. This crossover was also reflected in changes of the cluster structure, the fractal dimension decreasing as the clusters grew in size [6(c)]. The region of slow, reaction-limited growth coincides with nonscaling of $S(q, t)$.

Now RLCA is observed at all times in our experiments for lower salt molarities [6]. Figure 5 shows a typical sequence of images from such an experiment. Clusters of all sizes up to a time-dependent maximum coexist. This contrasts with the behavior in experiments at higher salt molarities, where the clusters are much more uniformly sized and spaced (Fig. 1). Despite the suggestion [10] that for RLCA $S(q, t)$ should lack peaks, in the present work peaks were observed at most times, suggesting that there is a most probable cluster separation (cf. Fig. 6). However, these $S(q, t)$ cannot be scaled onto a single curve for any value of the exponent d in Eq. (1).

It may thus be that the failure of Furukawa-like scaling at early times in experiments at high subphase salt concentrations connects with the absence of such scaling for RLCA.

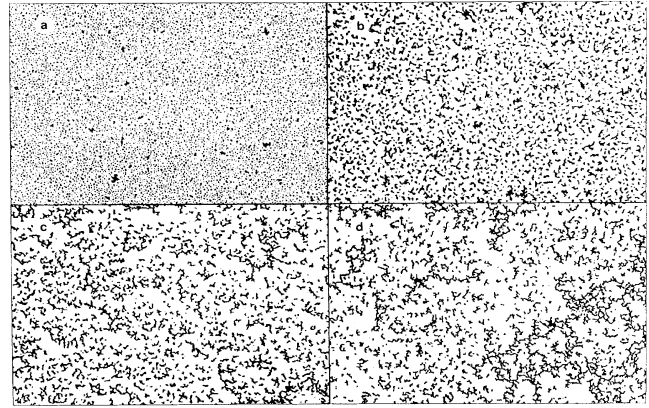


FIG. 5. As Fig. 1, but for substrate molarity $0.25M$: times (a) 75, (b) 270, (c) 315, and (d) 330 min. The polydispersity characteristic of RLCA is apparent.

$P(x)$ does not scale as $S(q, t)$. However, the distributions of Fig. 2 superimpose reasonably well if plotted as $x_m P(x/x_m)$: Compression of the abscissa by x_m is balanced by a similar expansion of the ordinates to retain the normalization of the distributions. In this sense $P(x)$ retains a constant shape for DLCA. This is not so for RLCA (Fig. 6), where the shape of $P(x)$ does change as aggregation proceeds. Specifically, for RLCA there always seems to be a significant population at small x even when the peak of $P(x)$ has moved substantially: $P(x)$ broadens but does not shift bodily as in DLCA (Fig. 2).

The kinetics described above arise from a low particle-particle bonding probability. We believe that this is due to significant residual electrostatic charges on the particles, relatively insensitive to screening, even by high substrate salt molarities [12]. However, as aggregation proceeds, the increasing number of possible contact points of large clusters with other particles or clusters will cause the effective probability of irreversible bonding to become significant [6(c)]. For lower salt concentrations the repul-

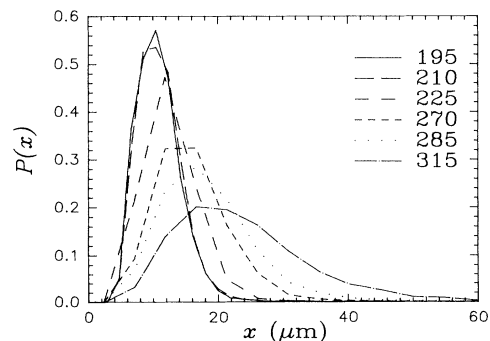


FIG. 6. Probability distributions of nearest neighbor separations for the monolayer of Fig. 5, based on 3741, 3617, 2772, 1762, 1339, and 801 clusters (for increasing times as legend).

sion will be greater, giving a smaller sticking probability, which may be so low that aggregation will preferentially involve only the largest clusters, leading to a polydisperse cluster size distribution (RLCA). The rather lower electrostatic repulsions at high molarities would reduce this tendency for only the larger clusters to interact, leading to a more monodisperse cluster size distribution (DLCA-like).

Why does DLCA-like behavior lead to Furukawa-like scaling? Previous studies [6(b)] have shown that the onset of rapid aggregation coincided with the appearance of large clusters. Apparently the rapid disappearance of small clusters in DLCA arises because they are mopped up by the large clusters, rather than aggregating with other small clusters. This, together with the residual electrostatic repulsion, would lead to depletion zones around the large clusters, the consequent spatial correlations between the clusters in DLCA leading to the scaling of $S(q, t)$. These inferences are supported by the distributions of nearest neighbor cluster separations. $P(x)$ moves bodily to larger x as DLCA proceeds, indicating the disappearance of clusters close to the larger ones, whereas for RLCA significant numbers of small separations persist until the entire colloidal monolayer gels.

The present results tend to support the hypothesis that Furukawa-like scaling is a general description of a wide variety of aggregation processes in colloids with attractive interactions [13].

This work has been supported by the SERC.

- [1] P. Meakin, in *Phase Transitions and Critical Phenomena*, edited by C. Domb and J.L. Lebowitz (Academic, New York, 1988), Vol. 12, p. 335.
- [2] M. Carpineti and M. Giglio, *Phys. Rev. Lett.* **68**, 3327 (1992).
- [3] E.g., J.S. Huang, W.I. Goldberg, and A.W. Bjerkaas, *Phys. Rev. Lett.* **32**, 921 (1974); S. Katano and M. Iizumi, *ibid.* **52**, 835 (1984); P. Wiltzius, F.S. Bates, and W.R. Heffner, *ibid.* **60**, 1538 (1988); P. Wiltzius, F.S. Bates, S.B. Dierker, and G.D. Wignall, *Phys. Rev. A* **36**, R2991 (1987).
- [4] H. Furukawa, *Adv. Phys.* **34**, 703 (1985); K. Binder and D. Stauffer, *Phys. Rev. Lett.* **33**, 1006 (1974); J. Marro, J.L. Lebowitz, and M.H. Kalos, *ibid.* **43**, 282 (1979).
- [5] D. Fritter, C.M. Knobler, and D.A. Beysens, *Phys. Rev. A* **43**, 2858 (1991).
- [6] (a) D.J. Robinson and J.C. Earnshaw, *Phys. Rev. A* **46**, 2045 (1992); (b) **46**, 2055 (1992); (c) **46**, 2065 (1992).
- [7] A.J. Hurd, *J. Phys. A* **18**, L1055 (1985).
- [8] F.P. Preparata and M.I. Shamos, *Computational Geometry* (Springer-Verlag, New York, 1985), Chap. 4.
- [9] J.S. Langer, in *Solids Far from Equilibrium*, edited by C. Godrèche (Cambridge Univ. Press, Cambridge, 1991), p. 297.
- [10] J. Bibette, T.G. Mason, H. Gang, and D.A. Weitz, *Phys. Rev. Lett.* **69**, 981 (1992).
- [11] D. Asnaghi, M. Carpineti, M. Giglio, and M. Sozzi, *Phys. Rev. A* **45**, 1018 (1992).
- [12] D.J. Robinson and J.C. Earnshaw (to be published).
- [13] P.W. Rouw, A.T.J.M. Wouterson, B.J. Ackerson, and C.G. de Kruif, *Physica (Amsterdam)* **156A**, 876 (1989).